Thermodynamics of Lithium Storage at Abrupt Junctions: Modeling and Experimental Evidence

Lijun Fu,* Chia-Chin Chen, Dominik Samuelis, and Joachim Maier†
Max Planck Institute for Solid State Research, Heisenbergstrasse 1, 70569 Stuttgart, Germany
(Received 30 September 2013; published 19 May 2014)

We present the thermodynamic modeling and experimental evidence of the occurrence of lithium storage at abrupt junctions, which describes the transition from an electrostatic capacitor to a chemical capacitor. In both $Ru:Li_2O$ and Ni:LiF systems, the functionalities and extracted parameters are in good agreement with the thermodynamic model, based on the dependence of the storage capacity on open-circuit voltage. Moreover, it is set out that a complete understanding of a conventional storage mechanism requires unifying both the space charge and bulk storage for a nanocrystalline electroactive electrode.

DOI: 10.1103/PhysRevLett.112.208301 PACS numbers: 82.47.Aa, 05.70.Np, 68.35.Md, 73.40.Ns

Chemical energy storage is one of the key processes for our society. In particular, electrochemical storage such as the storage of lithium in Li-based batteries provides the basis of a particularly efficient, powerful, and elegant reversible technology [1,2].

In this context, a novel storage mode was recently proposed [3–5]. This heterogeneous storage mode refers to interfaces and is directly connected with the existence of space charge zones. It culminates in the extreme case that a composite of two phases may store Li (i.e., $Li^+ + e^-$) even though none of the constituent phases (and also not the interfacial core itself) may store lithium themselves. This then happens in a "job-sharing" way: Li^+ is accumulated in one, the electron in the other phase. This may not only allow for a fast storage (Li^+ transport along one phase, e^- transport along the other); if the proportion of interfaces is high as it is in the case of nanocomposites such as in electrochemically prepared $Li_2O:Ru$, the Li uptake can also be substantial ($\sim 100\ mA\,h\,g^{-1}$ in $Li_2O:Ru$ nanocomposites) [2,4]. Such interfacial storage was also addressed in fluorides [6,7].

The mechanism is of fundamental importance for two reasons. (i) It describes the transition from an electrostatic capacitor to a chemical capacitor on a size reduction. At a large size, the system behaves as a supercapacitor where polarization only refers to the boundary. At a tiny size, the space charge layers overlap and in the atomistic limit the charge distribution approaches the homogeneous distribution that is met in chemical dissolution (insertion). (ii) Only the joint discussion of bulk and space charge storage allows for a complete description of general (electro-)chemical storage in nanocrystals where space charge zones may constitute a substantial fraction of the entire crystal, in particular, in the case of low Li concentration.

In this contribution, we give a clear thermodynamic evidence for the occurrence of such a job-sharing mechanism in two composite systems, $Li_2O:Ru$ and LiF:Ni. It is based on the dependence of the storage capacity on the open-circuit voltage. The good agreement with the thermodynamic considerations strongly corroborates the mechanism and excludes conventional bulk storage or the recombination of Li^+ and e^-.

Let us start with a discussion of conventional bulk storage (dissolution of lithium in a single phase). The bulk carrier concentration in dilute systems is calculated by considering the relevant mass action laws for the ionic and electronic charge carrier concentrations together with the electroneutrality equation (cf. appendix I in the Supplemental Material [8]). If majority and minority carriers can be distinguished, substantial simplifications are possible. The specific situation under concern is named the defect regime [9,10]. As far as Li incorporation into the lattice is concerned, it suffices to formulate the incorporation of Li^+ into interstitial sites whereby e^- are injected into the conduction band (characterized by the mass action constant $K_{Li} = ni/a_{Li}$, where $n \equiv$ concentration of conduction electrons e′, $i \equiv$ concentration of Li^+ interstitials $Li_i^\bullet$, $a_{Li} \equiv$ Li activity, the logarithm of which is linearly correlated with the chemical potential of lithium μ_{Li} or the cell voltage in a battery) (appendix I of the Supplemental Material [8]). Coupling this Li-incorporation equilibrium with internal electronic disorder equilibrium (electron-hole equilibrium, $K_B = np$, with $p \equiv$ hole concentration) and internal ionic disorder equilibrium (we assume Frenkel equilibrium, $K_F = iv$, with $v \equiv Li^+$-vacancy concentration) allows one to calculate the equilibrium charge-discharge relation cell voltage vs charge (Q). To give three examples: if intrinsic ionic (or electronic) disorder prevails, i.e., $i \simeq v$ (or $n \simeq p$) over the stoichiometric change introduced, the relation between charge stored simply follows as $Q_{Li} \propto a_{Li}$–consta_{Li}^{-1} and the relation between charge and voltage will be a sinh function. If Li excess (or deficiency) is prevailing over the intrinsic disorder, a case that is more relevant for perceptible storage, $Q_{Li} \propto a_{Li}^{1/2}$ (or $-a_{Li}^{-1/2}$), follows. While this is rather trivial and well settled [2], the analogous calculations for the job-sharing mechanism

at the interface of two phases α and β are more delicate.

Let us do this for the relevant case that significant storage of Li occurs in the form of interstitial and excess electrons. Then the heterogeneous storage reaction involving the phases α and β,

$$\mathrm{Li} \rightleftharpoons \mathrm{Li}_i^{\bullet}(\alpha) + \mathrm{e}'(\beta), \tag{1}$$

has to be considered. For dilute concentrations, a "mass action law" can be formulated as (see appendix I in the Supplemental Material [8]),

$$K_{\mathrm{Li}}^{\alpha/\beta} = i(\alpha) n(\beta) \kappa(\alpha,\beta) a_{\mathrm{Li}}^{-1}, \tag{2}$$

where two points are remarkable. First, the mass action constant is composed of contributions (standard chemical potentials μ^0, i.e., partial nonconfigurational free energy levels) from both phases [$\ln K_{\mathrm{Li}}^{\alpha/\beta} \propto \mathrm{const} + \mu_i^0(\alpha) + \mu_n^0(\beta)$]. Second, there is an additional term (κ) that takes account of the electrical potential (ϕ) drop between the two positions in α and β corresponding to the charging [$\kappa(\alpha,\beta) = \exp(\mathrm{e}(\phi_\alpha - \phi_\beta)/k_B T)$] [11]. A third point is worth mentioning with Eq. (2). Since $i(\alpha)$ and $n(\beta)$ can refer to different charge carrier regimes in α and β, the defect scenarios can be manifold. As concentrations and electrical potentials depend on each other, Poisson's equation needs to be considered in addition to the Boltzmann distribution already introduced when writing ideal mass action laws. The electrical potential drop $\phi_\alpha - \phi_\beta$ has three contributions: the space charge potentials in α and β, respectively, and the contact potential drop, i.e., the potential drop between the two outmost layers of α and β forming the contact (denoted by subscript 0). Let us first ignore the latter which is a good approximation for not too high $|Q_{\mathrm{Li}}|$ values. As a first case we consider the contact of two nonmetallic materials, and refer to the particularly relevant case that the excess charge dominates intrinsic disorder in both phases (i.e., $Q_{\mathrm{Li}^+}^{\alpha} \propto \int i^\alpha dx$; $Q_{e^-}^{\beta} \propto \int n^\beta dx$, where $Q_{\mathrm{Li}} \equiv Q_{\mathrm{Li}^+}^{\alpha} \equiv -Q_{e^-}^{\beta}$). This will be fulfilled at least for significant storage effects. The solution of the Poisson-Boltzmann equation then leads to two Gouy-Chapman profiles with $|Q^\alpha| \propto \sqrt{\epsilon^\alpha i_0^\alpha} \simeq \sqrt{\epsilon^\beta n_0^\beta} \propto |Q^\beta|$ [9–11], where the subscript 0 denotes the adjacent lattice planes at x_0^α and x_0^β. If we now formulate Eq. (1) for these positions and take account of $i_0^\alpha \simeq (\epsilon^\beta/\epsilon^\alpha) n_0^\beta$ according to Poisson's equation and global electroneutrality (ϵ: dielectric constant), we find $i_0^\alpha \propto n_0^\beta \propto a_{\mathrm{Li}}^{1/2}$ and hence $Q_{\mathrm{Li}} \propto a_{\mathrm{Li}}^{1/4}$, a strikingly different result from bulk storage (exponent 1/2). (Only extreme space charge overlap would change the exponents toward values of 1/2.) Importantly, if Li were introduced neutrally (in bulk or at interface) then the exponent would be +1, an even higher value. Note that 1/2 results from the dissociation of Li into two species (Li^+ and e^-) and 1/4 from the combination of dissociation and the diffuse double layer. As a second case, we refer to the realistic situation, where the electron-stabilizing phase β is a metal. Then the charge density on the metal site is concentrated on the first layer, thus $Q^\beta \propto n_0^\beta$. Instead of the power of 1/4, one then derives $Q_{\mathrm{Li}} \propto a_{\mathrm{Li}}^{1/3}$ [This is due to the fact that now $Q \propto i_0^{\alpha\,1/2} \propto n_0^\beta$ while Eq. (2) still holds true.] A smearing out of the surface charge (e.g., due to a tarnishing layer) will lead to a smaller exponent.

It is obvious that for large Q values, the missing potential drop between x_0^α and x_0^β characterized by κ will be of relevance (appendix II [8]). As long as one can model the region between the two layers at x_0^α and x_0^β by a gap with no charge stored and effective dielectric constant ϵ_{T}, Gauss' law yields

$$\kappa_0(\alpha,\beta) = \exp\frac{\Sigma e s}{\epsilon_T \epsilon_0 k_B T} \equiv \exp(\gamma Q) \tag{3}$$

(with Σ and s denoting positive integral charge density and contact distance). As a result we find for the Li-excess regime

$$\exp -\frac{eE}{k_B T} \propto a_{\mathrm{Li}} \propto Q^n \exp(\gamma Q), \tag{4}$$

with $n = 3$ or 4. In Eq. (4), E is, up to an additive constant due to normalization, identical with the cell voltage (appendix I [8]). Other cases can be treated similarly. In this equation, the constant γ contains the dielectric constant at the contact ϵ_T and contact distance s. For relatively small Q (high voltages), the factor Q^n in Eq. (4) will dominate, and for large Q (low voltages), the factor $\exp(\gamma Q)$ will dominate. Note that the behavior at high voltages (low storage) then emphasizes the diffuse double layer part, while the behavior at low voltages (high storage) corresponds to an electrostatic capacitance (voltage $\propto Q$). Equation (4) then shows also mathematically that the heterogeneous storage mode describes an intermediate between chemical and electrostatic storage. If, in a thought experiment, one shrinks the sizes of the phases α, β to atomistic dimensions, the field will disappear and $a_{\mathrm{Li}} \propto Q^2$ will originate in the limit of an extreme space charge overlap, hence yielding the result that is expected for a homogeneous situation. Note that for an extreme space charge overlap $Q_{\mathrm{Li}} \propto i_0^\alpha \propto n_0^\beta \propto a_{\mathrm{Li}}^{1/2}$; cf. Eq. (2).

Now let us discuss the experiments. We refer to two systems: (a) nanocomposites consisting of Ru and Li_2O, and (b) nanocomposites consisting of Ni and LiF. The nanocomposites are formed by electrochemical lithiation of RuO_2 and NiF_2, respectively. Both metals are able to store e^- but not Li^+, while LiF and in particular Li_2O can hardly accommodate e^- but easily accommodate Li^+ interstitially. This has also been confirmed by density functional theory (DFT) calculations [5,12]. Figure 1 shows the related discharge curve of RuO_2, displaying all the relevant storage modes: single phase storage in RuO_2 (I), two-phase storage

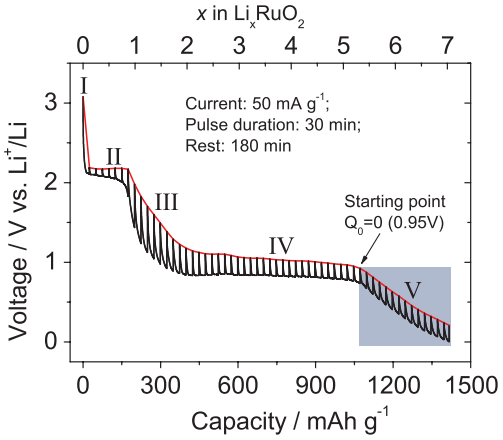

FIG. 1 (color). The open-circuit voltage of a battery with RuO_2 as a positive and Li as a negative electrode as a function of Li content, obtained by galvanostatic intermittent titration technique.

by forming $LiRuO_2$ (II), single phase storage therein (III), conversion to Li_2O:Ru (IV), and finally the regime of the interfacial storage (V) under concern here [4]. One recognizes a steep, almost linear, decay but with a perceptible bending.

Before we concentrate on these results, let us refer to the Ni:LiF system. Here the interfacial storage occurs at higher E values where we do not face the formation of passivation layers [6]. Owing to the voltage range, the storage is not so pronounced that we can identify a regime which is not substantially affected by the electrostatic storage part. As Fig. 2(a) shows, indeed a power law results with a slope of the predicted magnitude when the voltage is above 1.6 V vs Li/Li^+.

Now we extend the analysis to lower potentials where the rigid double layer part becomes perceptible. The experimental results shown in Fig. 2(b) again yield a power law in the range of small Q ($V > 1.60$ V) with the expected distinct deviation at lower voltage (large Q). However, if we apply the complete relation and plot $E + (4k_BT/e)\ln Q$ [cf. $F(Q, E)$ in Fig. 2(c)] vs Q, the whole curve linearizes with a γ value of the expected order of magnitude. Using reasonable values for s and ϵ_T, and referring to Q as charge per mass of the composite, we expect γ to be on the order of ~ 1 mA h g^{-1} (appendix II in the Supplemental Material [8]). n values lower than 3 give a distinctly worse fit; values higher than 4 would correspond to unrealistically low γ values (see Fig. S1 in the Supplemental Material [8]).

Let us now refer to Ru:Li_2O. The $\ln Q$ vs E curve for the relevant region (region V in Fig. 1) is displayed in Fig. S2 [8] for the first discharge with again a slope of the expected magnitude ($1/n \sim 0.3$), yet only at the high voltage side as expected from the above modeling. By exploiting Eq. (4), the whole curve linearizes (inset of Fig. S2 [8]), yet with too low γ values, coming from the irreversible formation of a passivation (SEI) layer in the first discharge process [4].

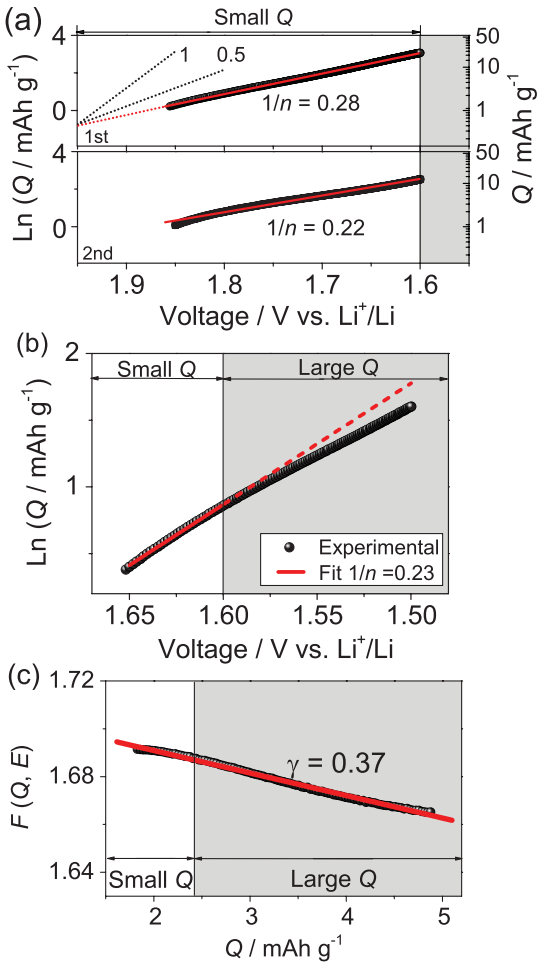

FIG. 2 (color). (a) Dependence of lithium interfacial storage on lithium activity in the first and second cycle in Ni:LiF nanocomposites. The Ni:LiF nanocomposites were electrochemically synthesized by inserting 2.2 Li into NiF_2 [13]. The initial point of the interfacial storage is not precisely known. Variation of the initial point in the range of $\pm 10\%$ of the total Q [14] shows that the slope is not much influenced; the $1/n$ value varies by not more than 0.05. It has to be noted that the results for the second cycle are more reliable, as the first discharge lacks of reversibility. (b) Dependence of lithium interfacial storage on lithium activity, indicating high (large Q) and low (small Q) storage regimes (fifth cycle). The linear plot reveals a power law with the expected exponent. (c) The fit derived from data in Fig. 2(b) displays the validity of Eq. (4) over the whole Q range for Ni:LiF. The y axis refers to $F(E, Q) = [E + n(k_BT/e)\ln(Q/\text{mAh g}^{-1})]/\text{V}$, here with $n = 4$. All dashed lines are shown for comparison. Bold red line is fitted; black line refers to experiment data.

In order to be able to draw more reliable conclusions on this system, (i) the cells have been cycled various times to obtain a stationary passivation layer and (ii) a fairly high current of 600 mA g^{-1} is applied. This leads, on the one hand, to greater overvoltage but simultaneously we expect to filter out the fast interfacial mechanism and to depress "parasitic" effects. Indeed, e.g., for the tenth cycle in the Li_2O:Ru case, the degree of reversibility is remarkable.

The remaining hysteresis between charging and discharging can be easily attributed to unavoidable internal resistances (Fig. 1), which do not influence strongly the applicability of Eq. (4) (if constant, they would only affect additive terms). Figure 3(a) shows the $\ln Q$ vs E plot for Li_2O:Ru. First, we notice that the exponents develop toward the right magnitude only for high voltages as expected. Second, and importantly, exploiting Eq. (4) by considering the $E + (nk_BT/e)\ln Q$ vs Q plot, the whole curve linearizes very nicely with slopes (γ) of the expected magnitude [Fig. 3(b)]. According to the voltage range, the diffuse part is only marginally observed in the limit of small Q values. Hence, differences in the fit quality only appear there. Best fits are obtained for n between 3 and 4 (Fig. S3 in the Supplemental Material [8]).

Evidently, we presented two compositions fulfilling the job-sharing model: the Li_2O:Ru case where the rigid double layer part is pre-eminent and the Ni:LiF case in which both contributions, the diffuse and rigid part, are of significance.

In view of the unavoidable complexity of the nanocomposites, the above results can be considered to be an excellent corroboration of the model. The space charge storage may also be relevant as far as the usually present passivation film (SEI) is concerned. As these passivation layers typically consist of Li ion but electron blocking compounds, interfaces of the passivation layers with metal or carbon, usually present at current collectors, can give rise to reversible excess storage as well [15].

A further important consequence of the consideration of space charges in the context of mass storage is achieving a unified understanding of the thermodynamic situation.

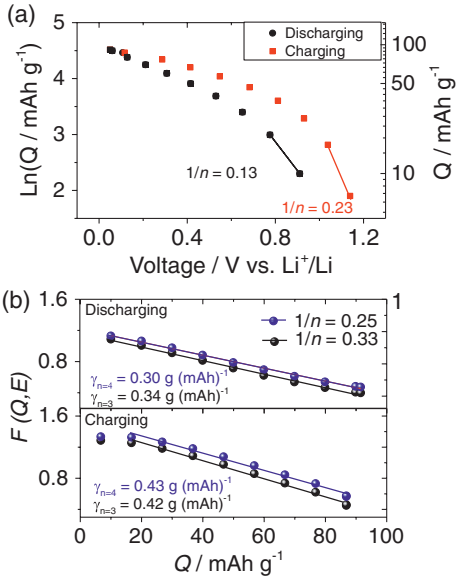

FIG. 3 (color). (a) Dependence of lithium interfacial storage on lithium activity in Ru:Li_2O nanocomposites (tenth cycle). (b) Dependence of $E + (nk_BT/e)\ln Q$ on interfacial storage Q, taking account of both chemical and electrostatic storage [14].

Every ionic crystal consists of both bulk and space charge zones, the latter being particularly relevant for nanocrystals which are preferably used for battery electrodes owing to the short diffusion length. Hence, only a comprehensive modeling of the combined bulk-space charge problem allows the calculation of the total concentration profiles as functions of lithium activity. This is overlooked in the battery community research, only in the context of ion transport, analogous considerations have been reported: in silver halides, boundary concentration and conductivities have been discussed as a function of silver activity [16,17] or in the context of nanocrystalline perovskite oxide as a function of oxygen partial pressure [18].

Figure 4 shows—for low Li activities—along with expected carrier concentration profiles, a sketch of Li storage in a nanocrystal of an electroactive material that can store Li in bulk and subsurface and for which Li^+ interstitials and excess electrons are the prevailing charge carriers. At low storage [low a_{Li}, Fig. 4(a)], the space charge zones are rather extended; at high storage [high a_{Li}, Fig. 4(b)], the space charge zones become very thin according to increased screening by higher defect concentrations. Also the integral charge density is smaller if normalized to the bulk storage, not because of the smaller Debye length (influence of bulk concentration cancels in the product of effective width and effective concentration) but because of $Q/Q_\infty \propto a_{Li}^{[(1/n)-(1/2)]}$, $3 < n < 4$, expressing that space charge storage, even though increasing, becomes less relevant when compared to the bulk contribution. These space charge profiles will be highly relevant for both transport and charge transfer kinetics.

In short, the thermodynamics of the novel job-sharing mechanism of electrochemical storage are considered and the equilibrium voltage vs charge curve discussed. We show that in spite of the complexity of the interfacial distribution, the functionality and the magnitude of the extracted parameters are in good agreement with the model.

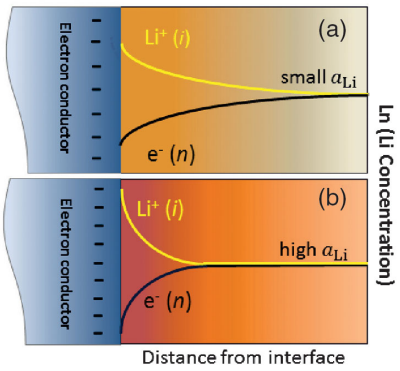

FIG. 4 (color). Sketch of Li storage in a nanocrystalline electroactive material which can store Li in bulk and subsurface at both (a) small and (b) high a_{Li}. Higher storage increases both bulk and space charge storage, but the latter to a lesser degree. In addition, the profiles narrow owing to storage screening.

This strongly corroborates the heterogeneous storage model (Li^+ and e^- separated by the phase contact) and excludes usual bulk storage or Li^+/e^- recombination. We also emphasize that only the unified treatment of space charge and bulk storage, which is possible along the described lines, allows for a detailed understanding of the conventional storage mechanisms if nanocrystals are employed.

*l.fu@fkf.mpg.de
†s.weiglein@fkf.mpg.de

[1] M. Armand and J. M. Tarascon, Nature (London) **451**, 652 (2008).
[2] J. Maier, Angew. Chem., Int. Ed. **52**, 4998 (2013).
[3] J. Jamnik and J. Maier, Phys. Chem. Chem. Phys. **5**, 5215 (2003).
[4] P. Balaya, H. Li, L. Kienle, and J. Maier, Adv. Funct. Mater. **13**, 621 (2003).
[5] Y. F. Zhukovskii, P. Balaya, E. A. Kotomin, and J. Maier, Phys. Rev. Lett. **96**, 058302 (2006).
[6] P. Liao, B. L. MacDonald, R. A. Dunlap, and J. R. Dahn, Chem. Mater. **20**, 454 (2008).
[7] X. Q. Yu, J. P. Sun, K. Tang, H. Li, X. J. Huang, L. Dupont, and J. Maier, Phys. Chem. Chem. Phys. **11**, 9497 (2009).
[8] See the Supplemental Material at http://link.aps.org/supplemental/10.1103/PhysRevLett.112.208301 for electrochemical thermodynamics (Appendix I), assessment of γ (Appendix II), and $F(Q, E)$ fits (Fig. S1–S3).
[9] J. Maier, *Physical Chemistry of Ionic Materials: Ions and Electrons in Solids* (Wiley, New York, 2004).
[10] F. A. Kroger, *The Chemistry of Imperfect Crystals* (North-Holland, Amsterdam, 1964).
[11] J. Maier, Ber. Bunsenges. Phys. Chem. **89**, 355 (1985).
[12] Y. F. Zhukovskii, P. Balaya, M. Dolle, E. A. Kotomin, and J. Maier, Phys. Rev. B **76**, 235414 (2007).
[13] H. Li, P. Balaya, and J. Maier, J. Electrochem. Soc. **151** A1878 (2004).
[14] Note that the terms low and high storage refer to charge per area. This should not be confused with the observed values of charge per mass plotted, e.g., in Figs. 2 and 3, that vary with the experimentally determined interfacial area. This interfacial area varies from experiment to experiment.
[15] J.-Y. Shin, D. Samuelis, and J. Maier, Adv. Funct. Mater. **21**, 3464 (2011).
[16] J. Maier, Phys. Chem. Chem. Phys. **11**, 3011 (2009).
[17] J. Maier, Nat. Mater. **4**, 805 (2005).
[18] P. Lupetin, G. Gregori, and J. Maier, Angew. Chem., Int. Ed. **49**, 10123 (2010).